

Photonic crystal band-stop filter with monomode resonator

B. LAZĂR, P. STERIAN*

Academic Center for Optical Engineering and Photonics, Faculty of Applied Sciences, University "Politehnica" Bucharest, Romania

In this paper, the behavior of a band-stop filter with monomode resonator, having potential applications in photonic crystal microcircuits, is studied using "coupled mode theory" which is an approximate method that allows relatively simple derivations of optimal design parameters. Coupled cavities appear everywhere in optical circuits. In many cases, they induce parasitic effects like important reflections back to the source. In other situations, if they are carefully tuned, optical devices consisting of micro cavities and guides can act as filters. The purpose of this article is to establish a procedure for designing efficient stop band filters with monomode, laterally coupled, cavities using a combination of analytical formula and numerical simulations.

(Received December 15, 2009; accepted January 20, 2010)

Keywords: Photonic crystals, Waveguides, Cavities, Reflection, Transmission coefficients

1. Introduction

Photonic crystals are periodic artificial nano structures which affect the propagation of electromagnetic waves in much the same way as the periodic potential in a semiconductor affects the electron motion, imposing allowed and forbidden electronic energy bands [5]. The existence of forbidden frequency bands inside photonic crystals leads to the possibility of constructing some micro optical devices like: highly efficient omnidirectional mirrors, low loss waveguides able to direct light even if sharp corners appear along their path [6] or miniature optical filters.

The current paper will deal just with a particular but important aspect of photonic crystal waveguide design, namely "the coupling of optical energy between a monomode cavity and an optical guide".

One way to directly analyze the behavior of waveguides, coupled with cavities, is to solve Maxwell Equations for a given photonic device (a part of space corresponding to the periodic dielectric pattern, possessing optical channels and cavities carved inside it) [7]. A popular method that is regularly employed in studying the electromagnetic wave propagation (solving Maxwell Equations) is FDTD (Finite Difference Time Domain). However, this mathematical procedure does not give direct indications regarding best configurations and optimal parameters. In most cases, it can be used just to verify some results obtained by other means. There are also situations when FDTD serves as a trial and error procedure but changing the value of some parameters and running the algorithm again and again is a time consuming and laborious undertaking, in many circumstances being hard to infer what values of input variables would lead to the desired behavior of the device under research.

In conclusion, an analytical formula, from which an optimal set of parameters could be easily deduced, is needed. One relatively simple approach [2], [8] is to consider an idealized configuration, like the one in Fig. 1, described by the system (1) - (2) where a number, varying from one to n , optical guides converge toward a resonant cavity that receives and, in the same time, leaks energy from and into these optical branches. Such a model, (1) - (2), is based on "coupled mode theory" and was developed having in mind ordinary guides without any relation to photonic crystals [1]. So, the association between this theoretical model and photonic guides coupled to resonant monomode cavities is a bit forced and any theoretical prediction obtained using (1) - (2) has to be validated with the help of FDTD simulations.

2. Simplified theoretical model for a unimode cavity coupled with n guides

The behavior of an optical monomode resonator, coupled to n input-output ports, can be described [1], [2] by the system of equations (1) - (2):

$$\frac{da(t)}{dt} = \left(j\omega_0 - \frac{1}{\tau} \right) a(t) + \underbrace{(C_1 \cdots C_n)}_{C^T} \underbrace{\begin{pmatrix} u_{1+}(t) \\ \vdots \\ u_{n+}(t) \end{pmatrix}}_{U_+(t)}, \quad (1)$$

$$\underbrace{\begin{pmatrix} u_{1-}(t) \\ \vdots \\ u_{n-}(t) \end{pmatrix}}_{U_-(t)} = \underbrace{\begin{pmatrix} m_{11} & \cdots & m_{1n} \\ \vdots & \ddots & \vdots \\ m_{n1} & \cdots & m_{nn} \end{pmatrix}}_{M} \underbrace{\begin{pmatrix} u_{1+}(t) \\ \vdots \\ u_{n+}(t) \end{pmatrix}}_{U_+(t)} + \underbrace{\begin{pmatrix} p_1 \\ \vdots \\ p_n \end{pmatrix}}_P a(t), \quad (2)$$

where a is the amplitude of the resonant mode with frequency ω_0 and lifetime τ , u_{i+} , u_{i-} , amplitudes of input, output signals respectively and C_i , p_i , m_i some complex constants.

The resonant mode is excited by input waves, u_{i+} , which couple to it with constants C_i . Also, the same mode, once created, starts to radiate energy coupling to the outputs with factors p_i . As a remark, the amplitude a is normalized in such a way that $|a(t)|^2 = E(t)$ (the energy inside the cavity).

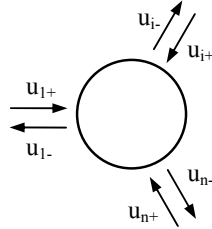


Fig. 1. Monomod cavity coupled with n input output ports.

The system (1) - (2) has also to satisfy the conservation of energy principle and the condition of being symmetrical with respect to time. The two restrictions lead to interdependences between: \mathbf{M} , \mathbf{p} and \mathbf{C} . In order to find the relationships between C_i , p_i and m_i , we will take all input signals u_{i+} , $i=1\dots n$ as being zero and the initial energy, inside the resonant cavity at $t=0$, will be considered $E(0)=|a(0)|^2$. In consequence, by solving (1), we get:

$$a(t) = a(0)e^{j\omega_0 t} e^{-\frac{t}{\tau}} \Rightarrow |a(t)|^2 = |a(0)|^2 e^{-\frac{2t}{\tau}}. \quad (3)$$

On the other hand, the decay rate of the energy must equal the power emitted by the cavity through the n ports:

$$\begin{aligned} \frac{d|a(t)|^2}{dt} &= -\frac{2}{\tau}|a(0)|^2 e^{-\frac{2t}{\tau}} = \\ &= -(u_{1-} \dots u_{n-})^* \begin{pmatrix} u_{1-} \\ \vdots \\ u_{n-} \end{pmatrix} = \\ &= -|a(0)|^2 e^{-\frac{2t}{\tau}} (p_1 \dots p_n)^* \begin{pmatrix} p_1 \\ \vdots \\ p_n \end{pmatrix} \end{aligned} \quad (4)$$

Therefore,

$$(p_1 \dots p_n)^* \begin{pmatrix} p_1 \\ \vdots \\ p_n \end{pmatrix} = \frac{2}{\tau}, \text{ or } (p_1 \dots p_n) \begin{pmatrix} p_1 \\ \vdots \\ p_n \end{pmatrix}^* = \frac{2}{\tau}. \quad (5)$$

As all input signals are considered zero, the equation (2) can be simplified to (6),

where $a(t)$ has been replaced by its particular expression in (3).

$$\begin{pmatrix} u_{1-}(t) \\ \vdots \\ u_{n-}(t) \end{pmatrix} = a(0)e^{j\omega_0 t} e^{-\frac{t}{\tau}} \begin{pmatrix} p_1 \\ \vdots \\ p_n \end{pmatrix}. \quad (6)$$

The process, described before, where the resonant cavity radiates its energy through output channels must be reversible. In other words, if the system is excited with the signal given by (6) reversed in time [1] (see (7))

$$\begin{pmatrix} u_{1+}(t) \\ \vdots \\ u_{n+}(t) \end{pmatrix} = a(0)e^{j\omega_0 t} e^{\frac{t}{\tau}} \begin{pmatrix} p_1 \\ \vdots \\ p_n \end{pmatrix}^*, \quad (7)$$

the energy must accumulate inside the cavity till $E(0)=|a(0)|^2$. Therefore if (7), is plugged as input signal, u_{i+} , in (1), the following equation is obtained:

$$\begin{aligned} \frac{da(t)}{dt} &= \left(j\omega_0 - \frac{1}{\tau} \right) a(t) + \\ &+ (C_1 \dots C_n) a(0) e^{j\omega_0 t} e^{\frac{t}{\tau}} \begin{pmatrix} p_1 \\ \vdots \\ p_n \end{pmatrix}^*, \end{aligned} \quad (8)$$

whose solution is:

$$a(t) = \frac{1}{2} a(0) e^{j\omega_0 t - \frac{t}{\tau}} \left((C_1 \dots C_n) \begin{pmatrix} p_1 \\ \vdots \\ p_n \end{pmatrix}^* \tau \left(e^{\frac{t}{\tau^2}} - 1 \right) + 2 \right). \quad (9)$$

If the time derivative of $|a(t)|^2$ is taken, then:

$$\frac{d|a(t)|^2}{dt} \Big|_{t=0} = \frac{2}{\tau} |a(0)|^2 \left((C_1 \dots C_n) \begin{pmatrix} p_1 \\ \vdots \\ p_n \end{pmatrix}^* \tau - 1 \right). \quad (10)$$

On the other hand, the rate of energy increase, inside the cavity, must equal the absorbed power through the n ports:

$$\frac{d|a(t)|^2}{dt} \Big|_{t=0} = |a(0)|^2 e^{-\frac{2t}{\tau}} (p_1 \dots p_n)^* \begin{pmatrix} p_1 \\ \vdots \\ p_n \end{pmatrix} \Big|_{t=0}. \quad (11)$$

From (10) and (11) it follows that:

$$(C_1 \dots C_n) \begin{pmatrix} p_1 \\ \vdots \\ p_n \end{pmatrix}^* = \frac{2}{\tau}. \quad (12)$$

From (12) and (5) it becomes evident that:

$$(C_1 \dots C_n) = (p_1 \dots p_n), \quad (13)$$

which shows that coefficients C_i and p_i can not be chosen at random but must be equal to each other.

Now, we will take a closer look at the elements of matrix \mathbf{M} . They can be found from the condition of zero

$$0 = \begin{pmatrix} m_{11} & \cdots & m_{1n} \\ \vdots & \ddots & \vdots \\ m_{n1} & \cdots & m_{nn} \end{pmatrix} a(0) e^{j\omega_0 t} e^{\frac{t}{\tau}} \begin{pmatrix} p_1 \\ \vdots \\ p_n \end{pmatrix}^* + \frac{1}{2} a(0) e^{j\omega_0 t - \frac{t}{\tau}} \left(C_1 \cdots C_n \begin{pmatrix} p_1 \\ \vdots \\ p_n \end{pmatrix} \tau \left(e^{\frac{t^2}{\tau^2}} - 1 \right) + 2 \begin{pmatrix} p_1 \\ \vdots \\ p_n \end{pmatrix} \right)_{t=0}, \quad (14)$$

which means that:

$$\begin{pmatrix} m_{11} & \cdots & m_{1n} \\ \vdots & \ddots & \vdots \\ m_{n1} & \cdots & m_{nn} \end{pmatrix} \begin{pmatrix} p_1 \\ \vdots \\ p_n \end{pmatrix}^* = - \begin{pmatrix} p_1 \\ \vdots \\ p_n \end{pmatrix}. \quad (15)$$

An important solution of (1) - (2) can be obtained by considering the input excitation as having the expression:

$$\begin{pmatrix} u_{1+}(t) \\ \vdots \\ u_{n+}(t) \end{pmatrix} = \begin{pmatrix} u_{1+} \\ \vdots \\ u_{n+} \end{pmatrix} e^{j\omega t} \Rightarrow \quad (16)$$

$$a = \frac{(C_1 \cdots C_n) \begin{pmatrix} u_{1+} \\ \vdots \\ u_{n+} \end{pmatrix}}{j(\omega - \omega_0) + \frac{1}{\tau}},$$

where u_{1+}, \dots, u_{n+} are known amplitudes.

$$r_i = \frac{u_{i-}}{u_{i+}} = \frac{m_{ii} j(\omega - \omega_0) + m_{ii} \frac{1}{\tau} + C_i C_i}{j(\omega - \omega_0) + \frac{1}{\tau}} \text{ or } R_i = \left| \frac{u_{i-}}{u_{i+}} \right|^2 = \frac{\left(m_{ii}(\omega - \omega_0) + |C_i|^2 \sin(2\varphi_{C_i}) \right)^2 + \left(m_{ii} \frac{1}{\tau} + |C_i|^2 \cos(2\varphi_{C_i}) \right)^2}{j(\omega - \omega_0) + \frac{1}{\tau}}, \quad (19)$$

$$t_{ij} = \frac{u_{j-}}{u_{i+}} = \frac{C_i C_j}{j(\omega - \omega_0) + \frac{1}{\tau}} \text{ or}$$

$$T_{ij} = \left| \frac{u_{j-}}{u_{i+}} \right|^2 = \frac{|C_i C_j|^2}{(\omega - \omega_0)^2 + \frac{1}{\tau^2}}; \quad i \neq j, \quad (20)$$

Taking into account that:

$$R_i + \sum_{\substack{j=1 \\ j \neq i}}^n T_{ij} = \frac{m_{ii}^2 (\omega - \omega_0)^2 + |C_i|^2 \sum_{j=1}^n |C_j|^2 + m_{ii}^2 \frac{1}{\tau^2} + 2m_{ii}(\omega - \omega_0) \sin(2\varphi_{C_i}) + 2m_{ii} \frac{1}{\tau} \cos(2\varphi_{C_i})}{(\omega - \omega_0)^2 + \frac{1}{\tau^2}} = 1 \quad (22)$$

The decay rate of the amplitude in the cavity, defined as the inverse of the lifetime corresponding to the resonant mode, can be written as the sum of decay rates corresponding to each port. Thus:

$$\frac{1}{\tau} = \sum_{i=1}^n \frac{1}{\tau_i} \text{ or } \frac{2}{\tau} = \sum_{i=1}^n \frac{2}{\tau_i}. \quad (23)$$

radiation at $t=0$. Therefore, the equation (2) where the input is the signal from (7) and $a(t)$ is the

solution of (8) (see the explicit formula (9)); must have the left member null at $t=0$. Thus:

By plugging (12) in (2), the output amplitudes take the form (17):

$$\begin{pmatrix} u_{1-} \\ \vdots \\ u_{n-} \end{pmatrix} = \begin{pmatrix} m_{11} & \cdots & m_{1n} \\ \vdots & \ddots & \vdots \\ m_{n1} & \cdots & m_{nn} \end{pmatrix} + \frac{\begin{pmatrix} C_1 \\ \vdots \\ C_n \end{pmatrix} (C_1 \cdots C_n)}{j(\omega - \omega_0) + \frac{1}{\tau}} \begin{pmatrix} u_{1+} \\ \vdots \\ u_{n+} \end{pmatrix}. \quad (17)$$

The expression (17) is useful for calculating reflection and transmission coefficients. Therefore, by considering just one port excited at a time, the input amplitudes corresponding to the other $n-1$ ports being zero, (17) can be rewritten as follows:

$$\begin{pmatrix} u_{1-} \\ \vdots \\ u_{i-} \\ \vdots \\ u_{n-} \end{pmatrix} = \begin{pmatrix} 0 \\ \vdots \\ m_{ii} u_{i+} \\ \vdots \\ 0 \end{pmatrix} + \frac{C_i u_{i+}}{j(\omega - \omega_0) + \frac{1}{\tau}} \begin{pmatrix} C_1 \\ \vdots \\ C_i \\ \vdots \\ C_n \end{pmatrix}, \quad (18)$$

from which, R and T can be calculated.

(see (12), (13)), and using (19), (20) the equality reflection + transmission = 1 is verified as can be seen in (22).

From (21) and (23) it follows that:

$$\sum_{i=1}^n \frac{2}{\tau_i} = \sum_{i=1}^n |C_i|^2 \Rightarrow |C_i| = \sqrt{\frac{2}{\tau_i}}. \quad (24)$$

3. Stop band filter with monomod resonator. Numerical results.

The theory in the previous paragraph is general and can be applied to all sorts of optical devices where a monomode resonant cavity couples its energy to and from a number of guides. However, this general model is a simplification of reality and there is no guaranty it gives acceptable results for various particular situations. In consequence, any predictions of behaviors of a certain optoelectronic device, obtained by using the above described mathematical relations, have to be verified by solving Maxwell Equations using a numerical method like FDTD or by pure experimental means.

As an example, a monomod cavity laterally coupled to a photonic guide will be studied (Fig. 2, Fig. 3) [3], [4].

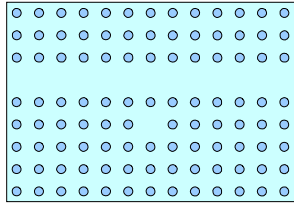


Fig. 2 Resonant cavity laterally coupled to a photonic guide.

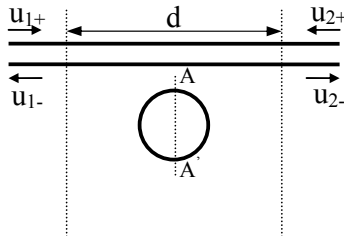


Fig. 3 Schematic representation of the microoptical device in Fig. 2.

According to the general theory in the previous paragraph, the optical device in Fig. 2, whose simplified theoretical model is given in Fig. 3, works as described by the equations (25) - (26) if the cavity is monomod.

$$\frac{da(t)}{dt} = \left(j\omega_0 - \frac{1}{\tau} \right) a(t) + \begin{pmatrix} C_1 & C_2 \end{pmatrix} \begin{pmatrix} u_{1+}(t) \\ u_{2+}(t) \end{pmatrix}, \quad (25)$$

$$\begin{pmatrix} u_{1-}(t) \\ u_{2-}(t) \end{pmatrix} = \begin{pmatrix} 0 & 1 \\ 1 & 0 \end{pmatrix} \begin{pmatrix} u_{1+}(t) \\ u_{2+}(t) \end{pmatrix} + \begin{pmatrix} C_1 \\ C_2 \end{pmatrix} a(t). \quad (26)$$

For calculating the reflection and transmission coefficients we will consider, as already explained,

$u_{2+}=0$ and $u_{1+}(t) = u_{1+}e^{j\omega t}$ which plugged in (25) lead to an expression of $a(t)$ identical to the one in (3). Also, by imposing the existence conditions from the previous paragraph, which in this particular case are:

$$(1) \begin{pmatrix} 0 & 1 \\ 1 & 0 \end{pmatrix} \begin{pmatrix} C_1^* \\ C_2^* \end{pmatrix} = - \begin{pmatrix} C_1 \\ C_2 \end{pmatrix} \quad (27)$$

and:

$$(2) \begin{pmatrix} C_1^* & C_2^* \end{pmatrix} \begin{pmatrix} C_1 \\ C_2 \end{pmatrix} = \frac{2}{\tau}, \quad (28)$$

the following equality is obtained:

$$|C_1|^2 = |C_2|^2 = 1/\tau. \quad (29)$$

The mathematical expressions of reflection and transmission coefficients can now be easily found using (3), the equation (26) and condition (29). Thus,

$$R = \left| \frac{u_{1-}}{u_{1+}} \right|^2 = \frac{1}{(\omega - \omega_0)^2 + \frac{1}{\tau^2}}, \quad (30)$$

$$T = \left| \frac{u_{2-}}{u_{1+}} \right|^2 = \frac{(\omega - \omega_0)^2}{(\omega - \omega_0)^2 + \frac{1}{\tau^2}}. \quad (31)$$

By making the notation, $\omega_l = 1/\tau$, (30) and (31) can be rewritten as:

$$R = 1 / \left[\left(\frac{\omega_0}{\omega_l} \right)^2 \left(\frac{\omega - \omega_0}{\omega_0} \right)^2 + 1 \right], \quad (32)$$

$$T = \left(\frac{\omega_0}{\omega_l} \right)^2 \left(\frac{\omega - \omega_0}{\omega_0} \right)^2 / \left[\left(\frac{\omega_0}{\omega_l} \right)^2 \left(\frac{\omega - \omega_0}{\omega_0} \right)^2 + 1 \right]. \quad (33)$$

The variation of T as a function of the relative shift in frequency with respect to ω_0 , for various values of the parameter ω_0/ω_l , is shown in Fig. 4, being a stop band characteristic.

As a remark, all the physical quantities in (32) and (33) are normalized to ω_0 in order the graphical representation in Fig. 4 be independent of the real values of ω , ω_0 , and τ . Therefore, in practical cases, if a particular value of ω_0 is known, the expression (33) (and its diagram in Fig. 4) helps finding the variation interval of ω and the values of $1/\tau$ for which T is maintained at reasonable low values.

In general, for rates $1/\tau$ small enough in comparison with ω_0 , $T(\Delta\omega/\omega_0)$ has a sharp variation and the transmission coefficient drops rapidly as $|\omega - \omega_0|$ gets larger and larger. If $\omega_l = 1/\tau$ has greater values, T becomes less dependent of the

difference $|\omega - \omega_0|$, staying close to zero for larger intervals of values.

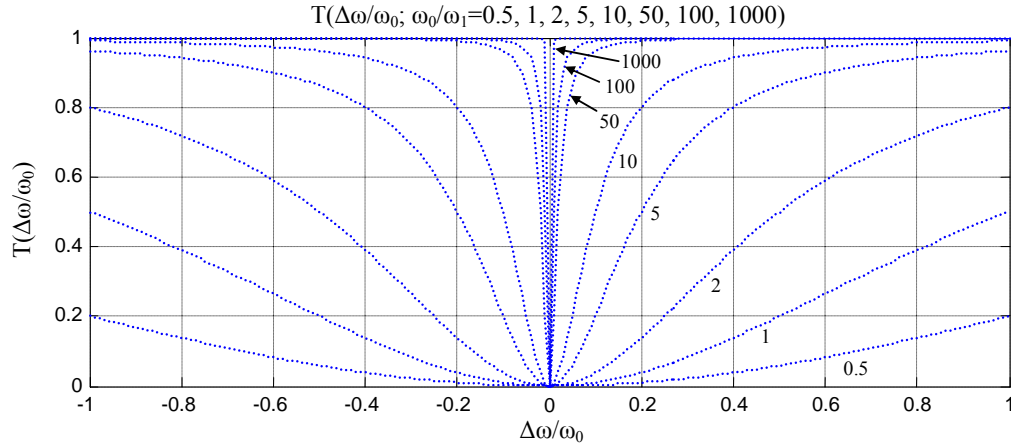


Fig. 4 The transmission coefficient T from (33) when ω_0/ω_1 vary from 0.5 to 1000.

The diagram in Fig. 4, obtained with the help of (33), looks pleasant, however, it remains to be seen if the real photonic device in Fig. 2 behaves as predicted by (33). Therefore, Maxwell Equations have to be solved

exactly for the cavity coupled with the photonic guide from Fig. 2. For this purpose the configuration shown in Fig. 7 (Fig. 2 extended over a large area of space) is chosen.

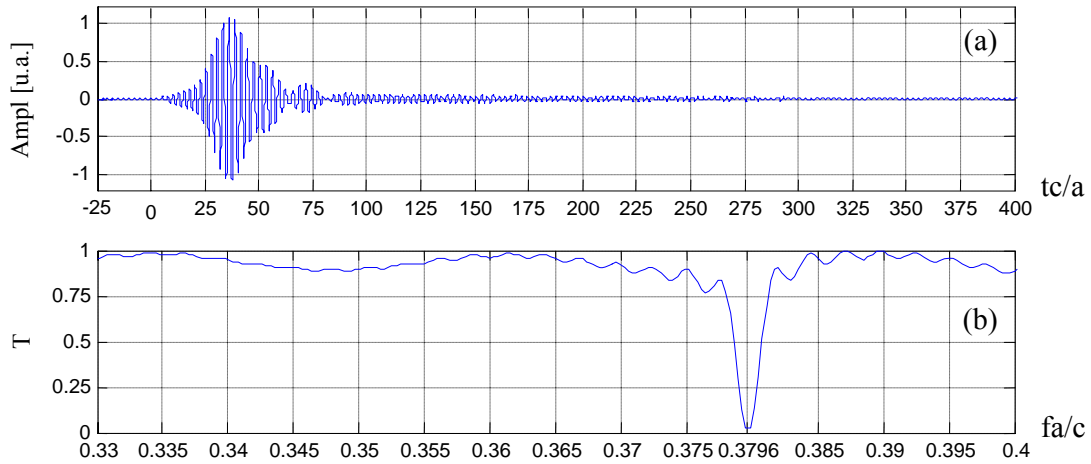


Fig. 5 a) The amplitude of the transmitted signal, measured in the point marked with \times situated above the resonant cavity in Fig. 7. b) $T(f) = E_t(f)/E_i(f)$. Total transmission = 0.9.

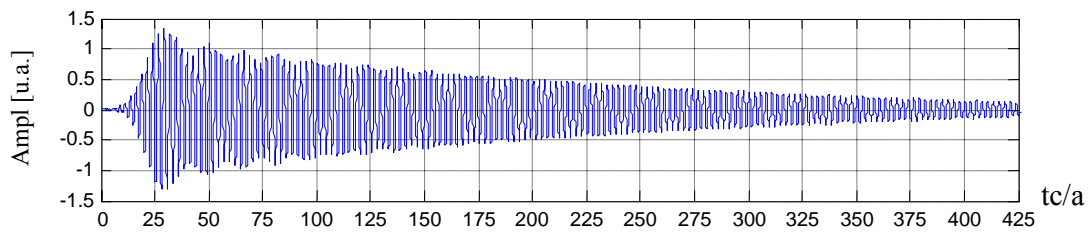


Fig. 6 The amplitude of the transmitted signal, measured in the point marked with \times situated above the resonant cavity in Fig. 7, for the case when a sinusoidal excitation having the frequency $f = 0.3796(c/a)$ acts in the location marked with $+$.

The building blocks of the crystal in Fig. 7 are characterized by $r=0.2a$, $\epsilon_{ra}=11.56$, $\epsilon_{rb}=1$, where r is the ray of the circular dielectric “atom”, ϵ_{ra} represents the relative electric permittivity of the “atom” and ϵ_{rb} the same dielectric constant but corresponding to the material that is found around the “atom” in the remaining of the cell.

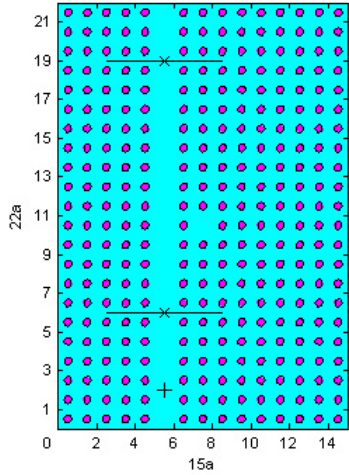


Fig. 7 Photonic optical guide laterally coupled to a monomod resonator.

The excitation source is a narrowband modulated pulse test signal, characterized by a uniform spectrum in the frequency range $[0.33(c/a), 0.4(c/a)]$ (where c is the speed of light in vacuum and a is the length of the side of each elementary square cell) and a maximum amplitude $A=2$ a.u.. The source is located at the bottom of Fig. 7, in the middle of the optical guide (the point marked with “+”).

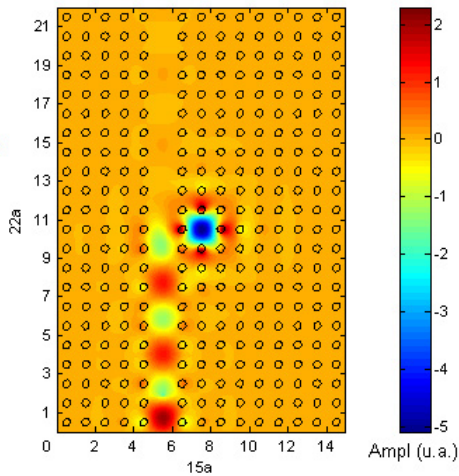


Fig. 8 The field map (the E_z component of the electromagnetic field) for the case when the source produces a sinusoidal excitation having the frequency $f=0.3796(c/a)$. The image corresponds to a moment after the stationary regime is reached.

The diagram in Fig. 6 demonstrates that the signal opposite to the source, with respect to the cavity, has a transitory regime which is an interval of time when the amplitude decreases with a rate dependent of the lifetime of the cavity. A stationary regime appears only after some time, the amplitude of the transmitted electric field stabilizing at a constant and close to zero value (Fig. 6).

As a note, regarding the evaluation of $T(f)=E_t(f)/E_i(f)$ in Fig. 5 (b), first of all, the entire incident energy, E_i , of the optical field (after the continuous regime is reached) that crosses the guide before the resonant cavity, is calculated, using the FDTD method. A function $E_i = E_i(f)$ is obtained. The same procedure is applied again, this time, for the transmitted energy, $E_t(f)$, in a cross section of the guide situated after the resonant cavity with respect to the source. Finally, $T(f)$ is obtained. Also, “total transmission = 0.9” (see Fig. 5 (b)) means that the entire energy (for all frequencies) transmitted in the guide beyond the cavity is 90% of the total incident energy.

4. Conclusions

The performances of a photonic crystal band-stop filter have been studied using a double approach. The first method, based on “coupled mode theory”, offers clear conditions for perfect transmission and zero reflection, being a powerful procedure for finding optimal parameters and explaining why the structure behaves like a band-stop filter. As can be seen by comparing Fig. 5 with Fig. 4, the band-stop transmission diagram, calculated with the help of “coupled mode theory”, is not identical with the one obtained using FDTD which means that the theoretical model described by (25) - (26) is not fully suitable for explaining the behavior of the real photonic device in Fig. 7. Despite the approximate nature of the method, the “coupled mode theory” proves to be a key tool that gives important information about the optimal configuration of photonic crystal based devices. It is true, because of its generality, “coupled mode theory” does not tell what measures have to be taken in order to attain the right coupling coefficients. Their optimal values have to be found using FDTD in a trial and error process.

Therefore, the analytical expression of T is only an approximation. Also, the values of $1/\tau$ need to be determined experimentally (numerically with the help of FDTD - Finite Difference Time Domain - procedure). However, the formula for T permits a quick identification of potential unsuitable values for $1/\tau$ (too small, big, etc.) and, in consequence, each τ can be adjusted accordingly, by inserting impurities of various diameters inside the cavity (a known procedure for modifying the emission absorption rate of the cavity). After a few FDTD simulations the right τ is obtained.

As a remark, before proceeding to design an optical device using “coupled mode theory” and FDTD the properties of the uniform photonic crystal (i.e. its frequency gaps) have to be determined because, outside this forbidden ranges, electromagnetic energy will penetrate in the body of the crystal rendering it useless. Also, the properties of the

particular optical guide and cavity, more precisely the number of modes, the field maps of each mode, etc., have to be determined. The analytical model based on “coupled mode theory” presented in this paper is only valid if the cavity supports just one mode or at least only one is excited by the optical field in the guide and the other modes remain always inactive.

References

- [1] H. A. Haus, “Waves and Fields in Optoelectronics”, Englewood Cliffs, NJ: Prentice-Hall, 1984.
- [2] Wonjoo Suh, Zheng Wang, IEEE Journal of Quantum Electronics, **40**(10), 1511 (2004).
- [3] Zheng Wang, Physical Review E **68**, 066616 (2003).
- [4] Wonjoo Suh, Applied Physics Letters, **84**, 24 (2004).
- [5] K. M. Ho, C. T. Chan, C.M. Soukoulis, Physical Review Letters, **65**(65), 3152 (1990).
- [6] C. Manolatou, Steven G. Johnson, Journal of Lightwave Technology, **17**(9), 1682 (1999).
- [7] Shangping Guo, Feng Wu, Sacharia Albin, Optics Express, **12**(8), 1741 (2004).
- [8] Chongjun Jin, Shanhui Fan, Shouzhen Han, Daozhong Zhang, IEEE Journal Of Quantum Electronics, **39**(1), 160 (2003).

*Corresponding author: sterian@physics.pub.ro